

# High spin state of Mn in an ideal monolayer on Ag(001)

P. Schieffer<sup>1</sup>, C. Krembel<sup>1</sup>, M.-C. Hanf<sup>1</sup>, M.-H. Tuilier<sup>1</sup>, P. Wetzel<sup>1</sup>, G. Gewinner<sup>1,a</sup>, and K. Hricovini<sup>2</sup>

<sup>1</sup> Laboratoire de Physique et de Spectroscopie Électronique<sup>b</sup>, Faculté des Sciences et Techniques,  
4 rue des Frères Lumière, 68093 Mulhouse Cedex, France

<sup>2</sup> Laboratoire pour l'Utilisation du Rayonnement Électromagnétique, Bâtiment 209 D, Centre Universitaire Paris-Sud,  
91405 Orsay Cedex, France, and LPMS, Université de Cergy-Pontoise, Neuville-sur-Oise, 95031 Cergy-Pontoise, France

Received: 4 May 1998

**Abstract.** We studied the magnetic properties of ultra-thin Mn films deposited on Ag (001) held at 80 K with soft X-ray absorption and magnetic circular dichroism. The observed shape and branching ratio of the Mn 2*p* absorption edge as a function of Mn coverage demonstrate that, up to  $\sim 0.9$  ML, the Mn adopts a stable high spin state similar to the Mn atom Hund's rule  ${}^6S_{5/2}$  ground state. Above this coverage a rapid transition from localized high spin to itinerant low spin behavior of the Mn 3*d* electrons is evidenced. Magnetic circular dichroism shows no sign of long range ferromagnetic order in these films at 80 K. The data, first confirm the large atomic-like local magnetic moment, and second are in line with the in-plane  $c(2 \times 2)$  antiferromagnetic order, reported recently (Phys. Rev. B **57**, 1141 (1998)), for Mn in the nearly ideal on-top Mn monolayer formed by 0.9 ML deposited at 80 K.

**PACS.** 75.70.Ak Magnetic properties of monolayers and thin films – 78.70.Dm X-ray absorption spectra – 78.20.Ls Magneto-optical effects

## 1 Introduction

Major changes in electronic structure and magnetic properties are expected when a transition metal is arranged in the two-dimensional form of an ultra-thin film as compared to its natural bulk phases. In a one-electron itinerant model a reduced coordination number and/or larger interatomic distance result in a reduced electronic band width and thus enhanced exchange splitting and magnetic moment. Yet, these changes are also accompanied by an enhancement of electron correlation effects that cannot be easily taken into account in the single particle approach. Nevertheless, theoretical work conducted in this framework apparently compares rather favorably with experiment for transition metal monolayers grown epitaxially on noble metal single crystal surfaces [1–4]. For even more dilute systems such as the ordered surface alloy  $c(2 \times 2)$  CuMn/Cu(001) marked discrepancies, for instance a considerably larger measured than calculated magnetic splitting, have been clearly evidenced recently [5]. As expected from density functional theory, better agreement is found for ground state properties such as the Mn atomic moment. Actually, the high localization of Mn 3*d* states in this system is demonstrated by the fact that the measured exchange splitting is comparable to the one observed for Mn impurities in Cu or Ag *i.e.* about 5 eV. The same

conclusion is arrived at from X-ray absorption spectroscopy (XAS) which shows an atomic-like  $\text{Mn}^{2+}$  ion  ${}^6S_{5/2}$  ground state [6,7]. Hence in such a dilute system with Mn–Mn interatomic distances as large as 3.61 Å an atomic model appears to be a better starting point to describe its properties and electron correlations are of primary importance. In the ordered surface alloy the electronic structure of the Mn is actually very similar to that of a single Mn impurity in a noble metal matrix. In our recent work [4] on Mn/Ag(001) system, this similarity is particularly evident for the ordered  $c(2 \times 2)$  MnAg/Ag(001) surface alloy formed at room temperature, *i.e.* valence band photoemission clearly demonstrates that the majority spin Mn 3*d* induced feature is essentially identical in shape and energy position to the one observed in dilute Ag based Mn alloys. Moreover, we succeeded in preparing a nearly perfect Mn monolayer by deposition of  $\sim 0.9$  ML Mn at 80 K on Ag(001) and found that the Mn 3*d* states still closely resemble those of an impurity in Ag matrix [4]. In this dense monolayer with  $p(1 \times 1)$  atomic order, the Mn–Mn spacing ( $d = 2.89$  Å) is much smaller than in the  $c(2 \times 2)$  MnCu/Cu(001) ( $d = 3.61$  Å) or  $c(2 \times 2)$  MnAg/Ag(001) ( $d = 4.07$  Å) surface alloys. This is quite remarkable since it means that in spite of enhanced direct Mn–Mn interaction ( $\sim 1$  eV) the 3*d* states remain highly localized and their atomic-like electronic structure is largely preserved. In this respect, we report here independent evidence of highly correlated Mn 3*d* electrons

<sup>a</sup> e-mail: g.gewinner@univ-mulhouse.fr

<sup>b</sup> UPRES A – CNRS 7014

in the (sub) monolayer range by means of soft X-ray absorption (XAS) measurements. The data are obtained from Mn ultra-thin films deposited on Ag(001) held at 80 K. According to previous work [4,8,9], the films grown under these conditions form an abrupt interface and their atomic structure is known with a good degree of confidence. This is an indispensable condition in order to establish a reliable relationship between atomic and electronic or magnetic structure of the Mn. Thus we are able to correlate a well marked transition from atomic to itinerant behavior of the Mn  $3d$  states with the formation of Mn-Mn nearest neighbor pairs with  $d \leq 2.89$  Å in the Mn deposit. Magnetic circular dichroism (XMCD) measurements performed on selected films exhibit no sign of ferro or ferrimagnetic long range order at 80 K. This is in line with the  $c(2 \times 2)$  antiferromagnetic superstructure observed by low energy electron diffraction (LEED) on the Mn monolayer [4] as well as the general tendency of antiferromagnetic coupling in transition metals with a nearly half filled  $3d$  shell.

## 2 Experimental

The films are grown in an UHV chamber at a pressure of about  $10^{-10}$  torr. The Ag(001) substrate prepared by standard methods [10] is kept at 80 K during deposition of the Mn at typical rates of  $\sim 0.3$  ML/min (1 ML equivalent to the Ag(001) surface atomic density) at a residual pressure below  $\sim 3 \times 10^{-10}$  torr. No O or C contamination was detectable by means of Auger or photoemission spectroscopy. According to previous work [4] the growth is pseudomorphic and nearly layer by layer up to  $\sim 0.9$  ML, where the film corresponds to a physical realization of an ideal Mn monolayer on Ag(001). At this stage there is only a small fraction of Mn in second layer positions and  $\sim 95\%$  of the Mn occupies the fourfold hollows of the Ag(001) surface [4]. Above 0.9 ML the fraction of second layer atoms increases rapidly as evidenced by X-ray photoelectron diffraction and the Mn interlayer spacing close to 1.9 Å in Mn bilayers, is reduced to  $\sim 1.66$  Å by 3–4 ML which corresponds to the spacing observed at larger coverages [9]. A metastable epitaxial Mn phase is formed in this way, that is body centered tetragonal (bct) with  $c/a \approx 1.15$ , lattice matched with Ag(001), and the interface is quite sharp [4,8,9]. Above  $\sim 6$  ML polycrystalline Mn  $\alpha$  tends to be formed but it is possible to grow thicker bct films if one initially condenses 3 ML at 80 K and then continues the growth with the sample heated at 300 K [9].

## 3 Results and discussion

All XAS data were obtained with the sample kept at 80 K at beam line SU 23 of the SUPERACO storage ring at Orsay. The measurements use the total electron yield by monitoring the sample drain current. In XMCD experiments, a magnetic field pulse up to 300 Oe was applied in order to align possible ferromagnetic domains. Measurements were also taken under an applied field of 200 Oe.

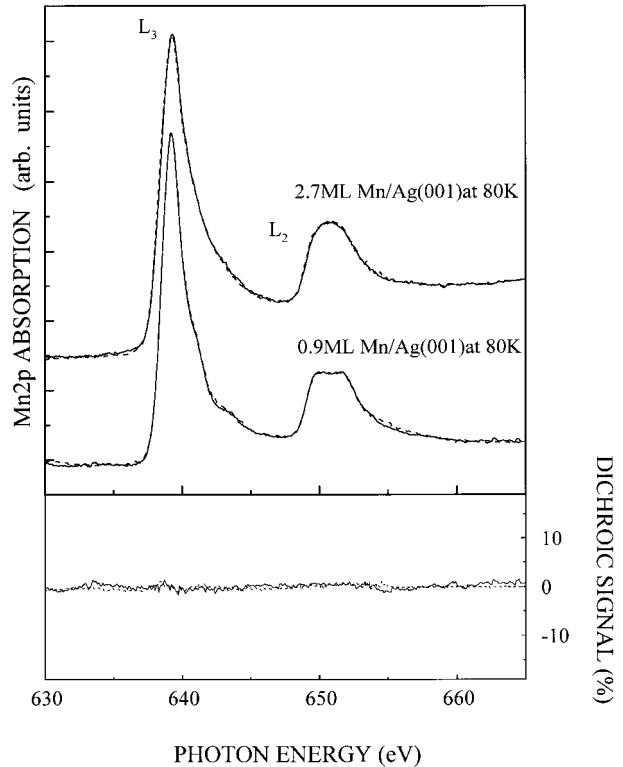


**Fig. 1.** Magnetic circular dichroism for 0.9 and 2.7 ML Mn on Ag(001) measured with  $\sigma+$  (full line) and  $\sigma-$  (dashed line) light.

Since nothing is known about orientation of easy magnetization axes, the field was applied along a direction rotated by  $\sim 45^\circ$  off surface normal. This also corresponds to the direction of incidence of the photon beam with a degree of circular polarization of  $\sim 70\%$ . In spite of various attempts, either in remanence or under applied magnetic field, at 80 K no X-ray helicity dependence of the absorption could be evidenced at any Mn coverage ranging from 0.3 ML up to  $\sim 10$  ML. Typical XMCD data are displayed in Figure 1 for 0.9 ML and 2.7 ML respectively. In both cases the XMCD signal is zero within experimental error. The absence of ferromagnetic long range order is not surprising at large coverages ( $\sim 10$  ML) since in bulk Mn phases coupling is antiferromagnetic with vanishing total moment per unit cell [11]. As expected, we find no sign of nonzero XMCD signal for 10 ML deposited at 80 K which results in a film mainly composed of polycrystalline stable Mn  $\alpha$  phase. The 2.7 ML film however consists of a metastable epitaxial bct Mn phase. According to previous work on Mn/Ag(001) superlattices [12], this kind of phase is believed to correspond to a stacking of ferromagnetic Mn(001) planes coupled antiferromagnetically along [001] direction. As observed no XMCD signal is expected at least at large coverages where interfacial effects can be neglected since this phase is also a antiferromagnet. Yet, the absence of dichroism for the 2.7 ML film is a more remarkable result since if the layered antiferromagnetic structure of bct Mn is preserved in ultra-thin films, the sum of the moments in the various Mn(001) planes is not,

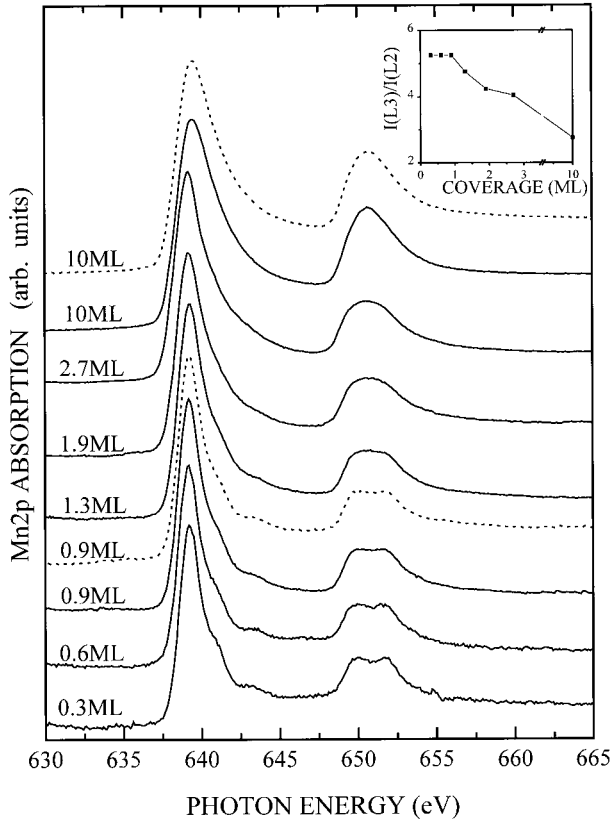


**Fig. 2.** Mn 2p absorption spectra as a function of Mn coverage in the 0.3–10 ML range for deposition at 80 K (full line) and at room temperature (dashed line). The inset show the evolution of the branching ratio *versus* coverage at 80 K.

*a priori*, zero. For instance in an ideal 3 ML film that keeps the bulk Mn bct magnetic structure, one naively expects ferrimagnetic behavior with resulting magnetization of the order of the one in a single (ferromagnetic) Mn(001) plane. Thus, the present observations indicate either that there is no magnetic long range order at all at 80 K in such ultrathin films, or that interfacial and surface effects conspire to adjust the magnitude and orientation of the magnetic moments of different inequivalent Mn in such a way that the total moment per unit surface cell cancels. Apparently a true antiferromagnetic structure tends to be always preserved in spite of strong changes in atomic structure (stable Mn  $\alpha$  *versus* metastable bct Mn) or film thickness. Similarly, the absence of XMCD in the monolayer range is in line with the conclusion arrived at in a previous LEED work. Indeed careful observations provide compelling evidence that the 0.9 ML film, which is a two dimensional square lattice arrangement of the Mn with  $a = 2.89 \text{ \AA}$ , exhibits long range in plane  $c(2 \times 2)$  antiferromagnetic order [4]. This kind of  $c(2 \times 2)$  superstructure is clearly observed in the 0.6–1.3 ML range. In the submonolayer range ( $< 0.6 \text{ ML}$ ) the possibility of superparamagnetism or antiferromagnetism with reduced critical temperature below 80 K cannot be ruled out on the basis of data at hand.

The absence of dichroism in Mn films on Ag(001) means that the  $L_{2,3}$  absorption edges measured with  $\sigma+$  and  $\sigma-$  light are identical and correspond to isotropic XAS data obtained with unpolarized light. The line shape of such spectra has been shown in previous work to yield valuable information on ground state properties such as d electron count and electronic structure and magnetic moments [13,14]. Figure 2 displays the evolution of the Mn  $L_{2,3}$  absorption edges as a function of Mn coverage in the 0.3–10 ML range. The spectra reveal two well marked lines that correspond to transitions into Mn 3d states that produce  $2p_{3/2}$  and  $2p_{1/2}$  core holes. For comparison the spectra are normalized to give the same intensity at the  $L_3$  line. As can be seen, the thick films ( $\sim 10 \text{ ML}$ ), irrespective of their detailed atomic structure (Mn  $\alpha$  or bct Mn), present the same broad “metallic” shape without any fine structure and the branching ratio defined as the intensity ratio  $I(L_3)/I(L_3) + I(L_2)$  is 0.69 *i.e.* approaches the statistical value of  $2/3$ . This line shape is characteristic of a low spin configuration with itinerant Mn 3d electrons. It is in sharp contrast with the line shape observed in the submonolayer range. For a coverage of 0.3 ML detailed structures can be seen, as well as a marked increase in relative intensity of the  $L_3$  line, that reflect an atomic-like  $3d^5$  ground state. This kind of spectrum has been observed before in  $c(2 \times 2)$  MnCu/Cu(001) and MnNi/Ni(001) surface alloys [6,7], dilute Mn in Ag [15] and submonolayer amounts of Mn on Fe(001) [16]. It is well described by atomic calculations based in the high spin Hund’s rule atomic  $^6S_{5/2}$  Mn ground state, allowing for a scaling of electrostatic interactions and some weight of the  $3d^6\bar{L}$  configuration in the ground state [15,17].  $\bar{L}$  denotes a hole in the ligand (Fe, Ag ...) that results from hopping into Mn 3d states. This ground state is characterized by a large spin local moment ( $\geq 4 \mu_B$ ) *i.e.* close to the free atom maximum. The most remarkable point here is that no major change in spectral shape takes place up to  $\sim 0.9 \text{ ML}$ , except for some blurring of the fine structure, such as a sizeable reduction in the dip between the two components of the  $L_2$  line. The branching ratio does not change within experimental error in this range (see inset in Fig. 2). Since a large branching ratio directly reflects the high spin ground state of the Mn [17] we must conclude that the latter persists up to  $\sim 0.9 \text{ ML}$  where a nearly ideal Mn monolayer is formed. Thus the XAS data clearly confirm the conclusion obtained in previous photoemission work [4], namely that Mn in a monolayer on Ag(001) is in a high spin state comparable to the one observed for a Mn impurity in Ag or a Mn adatom on Ag(001). The small spectral changes observed in submonolayer range with increasing coverage may reflect the enhanced lateral interaction between the Mn adatoms. Yet by 0.9 ML a small fraction of the Mn ( $\sim 5\%$ ) is in second layer positions. This results in Mn–Mn pairs with an interatomic distance of  $2.78 \text{ \AA}$ , *i.e.* markedly smaller than  $2.89 \text{ \AA}$ , the distance between nearest neighbors in the perfect monolayer [4], as well as in a larger mean number of the nearest neighbors. The strongly enhanced hybridization of the 3d states in this atomic environment appears to destroy the atomic like high spin state

of the Mn very effectively. Hence, growth imperfections, *i.e.* deviations from ideal layer by layer mode, may be responsible of or at least contribute to the blurring of the fine structure observed by 0.9 ML.

Actually, the very strong effect of the enhanced Mn–Mn interaction that appears when a substantial fraction of the second Mn atomic layer is occupied is demonstrated very clearly in Figure 2. In the 0.9–2.7 ML range the fine structure rapidly disappears and the spectrum acquires a typical “metallic” shape. The striking transition that mainly occurs in 0.9–2 ML range between atomic-like high spin and metallic low spin state is particularly evident when considering the evolution of the branching ratio which exhibits a sharp drop in this coverage range. Let us emphasize that this behavior of Mn when deposited on Ag(001) held at 80 K is in sharp contrast with the one reported for Mn on Fe(001) where a rapid evolution of the XAS spectra is observed in the submonolayer range [16]. The comparison is particularly relevant because both substrates have essentially the same surface lattice parameter *i.e.* in ideal monolayers the Mn–Mn nearest neighbor spacing is the same, about 2.89 Å. The present data for Mn/Ag(001) show that the increasing atomic coordination with Mn coverage in the submonolayer range does not result in a transition from highly localized to itinerant electrons, the high spin state being mainly preserved up to a complete (flat) monolayer where each Mn has 4 nearest neighbors at 2.89 Å. Possibly the transition from localized to delocalized behavior observed in the submonolayer range for Mn/Fe(001) reflects a non ideal growth of the Mn at room temperature (RT) such as formation of a surface alloy or Mn bilayer islands with enhanced Mn–Fe or Mn–Mn hybridization. In the Mn/Ag(001) case, formation of a  $c(2 \times 2)$  surface alloy definitely takes place when deposition of  $\sim 1$  ML is achieved at RT [4,10]. In Figure 2 we also show relevant XAS data for comparison. It is quite clear that Mn in this alloy exhibits the same high spin absorption spectrum than the on-top monolayer obtained by deposition of 0.9 ML at 80 K. Previous SEX-AFS studies reveal that in this surface alloy the nearest Mn–Mn interatomic distance is about 2.88 Å the same as Mn–Ag spacing and the Mn is confined to the two topmost atomic layers with an approximately  $\text{Mn}_{50}\text{Ag}_{50}$  stoichiometry [18]. Obviously, in spite of the increased Mn atomic coordination ( $\sim 4$  as opposed to 0 Mn nearest neighbors), a high spin state similar to the one for dilute Mn in Ag persists at the much larger 50% concentration in the surface alloy. In the Mn/Fe(001) case, Mn incorporated into the Fe substrate is expected to give rise to much larger hybridization and itinerant behavior since the nearest neighbor Mn–Fe distance should be  $\sim 2.50$  Å *i.e.* much shorter than in the MnAg alloy.

In conclusion, XAS experiments show that Mn in an ideal dense monolayer on Ag(001) preserves an atomic-like high spin state with large local magnetic moment ( $\sim 4 \mu_B$ ), similar to the one of a Mn adatom on or an impurity in Ag(001) substrate. The data indicate that there exists a critical Mn–Mn interatomic distance  $d \approx 2.89$  Å where (and beyond which) the high-spin ground state

becomes stable and shows little dependence on specific atomic environment for not too large ( $\leq 4$ ) Mn coordination numbers. Structures with higher Mn coordination (such as in metastable bct Mn or  $\alpha$ -Mn) invariably result in substantially reduced interatomic Mn–Mn distances and a sharp transition to a low spin state. This is completely in line with previous photoemission work [4] where it was found that the Mn 3d states and, in turn, the relevant magnetic splitting and local magnetic moment are fairly insensitive to changes in atomic structure provided that the nearest Mn–Mn interatomic distance remains large enough ( $d \geq 2.89$  Å). Finally XMCD measurements show no ferromagnetic long range order at 80 K in the ideal monolayer or at any coverage in the 0–10 ML range.

## References

1. C.L. Freeman, A.J. Fu, T. Oguchi, Phys. Rev. Lett. **54**, 2700 (1985); S. Blügel, Phys. Rev. Lett. **68**, 851 (1992).
2. W. Heinen, C. Carbone, T. Kachel, W. Gudat, J. Electron. Spectrosc. Rel. Phenom. **51** (1990) 701; F. J. Himpsel, *et al.*, Phys. Rev. B **49**, 14028 (1994).
3. C. Krembel, M.C. Hanf, J.C. Peruchetti, D. Bolmont, G. Gewinner, Phys. Rev. B **44**, 11472 (1991); G. Allan, Phys. Rev. B **44**, 13641 (1991).
4. P. Schieffer, C. Krembel, M.C. Hanf, G. Gewinner, Phys. Rev. B **57**, 1141 (1998) and Surf. Sci. **400**, 95 (1998).
5. O. Rader, W. Gudat, C. Carbone, E. Vescovo, S. Blügel, R. Kläsger, W. Eberhardt, M. Wuttig, J. Redinger, F.J. Himpsel, Phys. Rev. B **55**, 5404 (1997); Euro. Phys. Lett. **39**, 429 (1997).
6. W.L. O’Brien, J. Zhang, B.P. Tonner, J. Phys.-Cond. **5**, L515 (1993).
7. W.L. O’Brien, B.P. Tonner, Phys. Rev. B **51**, 617 (1995); Phys. Rev. B **50**, 2963 (1994).
8. W.F. Egelhoff Jr., I. Jacob, J.M. Rudd, J.F. Cochran, B. Heinrich, J. Vac. Sci. Technol. A **8**, 1582 (1990).
9. P. Schieffer, C. Krembel, M.C. Hanf, G. Gewinner, Surf. Sci. **402-404**, 318 (1998).
10. P. Schieffer, C. Krembel, M.C. Hanf, G. Gewinner, Phys. Rev. B **55**, 13884 (1997).
11. F. Süss, U. Krev, J. Magn. Magn. Mater. **125**, 351 (1993).
12. B.T. Jonker, J.L. Krebs, G. A. Prinz, Phys. Rev. B **39**, 1399 (1989).
13. B.T. Thole, P. Carra, F. Sette, G. Van Der Laan, Phys. Rev. Lett. **68**, 1943 (1992); P. Carra, B.T. Thole, M. Altarelli, X. Wang, Phys. Rev. Lett. **38**, 3158 (1993).
14. B.T. Thole, G. Van Der Laan, Phys. Rev. B **38**, 3158 (1988).
15. B.T. Thole, R.D. Cowan, G.A. Sawatzky, J. Finck, J.C. Fuggle, Phys. Rev. B **31**, 6856 (1985).
16. H.A. Dürr, G. Van Der Laan, D. Spanke, F.U. Hillenbrecht, N. B. Brookes, Phys. Rev. B **56**, 8156 (1997); J. Dressehaus *et al.*, Phys. Rev. B **56**, 5461 (1997).
17. G. van der Laan, B. T. Thole, Phys. Rev. B **43**, 13401 (1991).
18. P. Schieffer, M.H. Tuilier, C. Krembel, M.C. Hanf, G. Gewinner, D. Chandresris, H. Magnan, Phys. Rev. B **57**, 15507 (1998).